

Coupled abiotic-biotic cycling of nitrous oxide in tropical peatlands

Steffen Buessecker^{1†}, Analissa F. Sarno¹, Mark C. Reynolds¹, Ramani Chavan², Jin Park², Marc Fontánez Ortiz¹, Ana G. Pérez-Castillo³, Grober Panduro Pisco⁴, José David Urquiza-Muñoz^{5,6,7}, Leonardo P. Reis⁸, Jefferson Ferreira-Ferreira⁸, Jair M. Furtunato Maia^{9,10}, Keith E. Holbert¹¹, C. Ryan Penton¹², Sharon J. Hall¹, Hasand Gandhi^{13,15}, Iola G. Boëchat¹⁴, Björn Gücker¹⁴, Nathaniel E. Ostrom^{13,15}, Hinsby Cadillo-Quiroz^{1,2*}

¹ School of Life Sciences, Arizona State University, Tempe, Arizona, USA

² Bidesign Institute, Arizona State University, Tempe, Arizona, USA

³ Environmental Pollution Research Center (CICA), University of Costa Rica, Montes de Oca, Costa Rica

⁴ School of Forestry and Environmental Sciences, Ucayali National University, Ucayali, Peru

⁵ Laboratory of Soil Research, Research Institute of Amazonia's Natural Resources, National University of the Peruvian Amazon, Iquitos, Loreto, Peru

⁶ School of Forestry, National University of the Peruvian Amazon, Iquitos, Loreto, Peru

⁷ Department for Biogeochemical Processes, Max Planck Institute for Biogeochemistry, Jena, Germany

⁸ Mamiraua Institute for Sustainable Development, Amazonia, Brazil

⁹ Normal Superior School, Amazonas State University, Manaus, Amazonia, Brazil

¹⁰ National Institute of Amazonian Research, Manaus, Amazonia, Brazil

¹¹ School of Electrical, Computer and Energy Engineering, Arizona State University, Tempe, Arizona, USA

¹² College of Integrative Sciences and Arts, Arizona State University, Mesa, Arizona, USA

¹³ Department of Integrative Biology, Michigan State University, East Lansing, Michigan, USA

¹⁴ Applied Limnology Laboratory, Department of Geosciences, Federal University of São João del-Rei, São João del-Rei, Brazil

¹⁵ DOE Great Lakes Bioenergy Research Center, Michigan State University, East Lansing, Michigan, USA

[†] Current address: Department of Earth System Science, Stanford University, Stanford, California, USA

* Correspondence to: Hinsby Cadillo-Quiroz (hinsby@asu.edu)

37 **Abstract**

38 Atmospheric nitrous oxide (N₂O) is a potent greenhouse gas thought to be mainly
39 derived from microbial metabolism as part of the denitrification pathway. Here, we report that
40 in unexplored peat soils of Central and South America, N₂O production can be driven by abiotic
41 reactions ($\leq 98\%$) highly competitive to their enzymatic counterparts. Extracted soil iron
42 positively correlated with *in-situ* abiotic N₂O production determined by isotopic tracers.
43 Moreover, we found that microbial N₂O reduction accompanied abiotic production, essentially
44 closing a coupled abiotic-biotic N₂O cycle. Anaerobic N₂O consumption occurred ubiquitously
45 (pH 6.4-3.7), with proportions of diverse clade II N₂O-reducers increasing with consumption
46 rates. Our findings show denitrification in tropical peat soils is not a purely biological process,
47 but rather a “mosaic” of abiotic and biotic reduction reactions. We predict hydrological and
48 temperature fluctuations differentially affect abiotic and biotic drivers and further contribute to
49 the high N₂O flux variation in the region.

50 **Introduction**

51 The atmospheric accumulation of nitrous oxide (N₂O), a potent greenhouse gas, has
52 continued to increase^{1,2}, calling for a better mechanistic understanding of its sources and sinks.
53 Tropical soils are a major source of N₂O. The largest contribution to global N₂O flux, along
54 with the highest uncertainties, have been observed over South America³⁻⁵ with large flux
55 variations described in ground-based measurements from extensive peatlands of the Amazon
56 basin^{6,7}.

57 In waterlogged tropical peat soils, anoxic, reducing, humic acid-rich, and Fe-holding
58 conditions are favorable for the abiotic formation of N₂O⁸. Nitrous oxide can abiotically form
59 from the reduction of nitrite (NO₂⁻) via intermediary nitric oxide (NO), or hydroxylamine
60 (NH₂OH)⁹, both of which have typically low steady-state concentrations in soils.
61 Hydroxylamine conversion into N₂O relies on oxidants such as manganese (IV) minerals that
62 are unlikely to persist in sufficient levels in the reducing milieu of peat. Thus, peatlands would
63 generally favor the spontaneous chemical reduction of nitrogenous compounds – also called
64 chemodenitrification. Some environments appear to sustain abiotic N₂O production rates based
65 on dissolved Fe and Fe mineral phases¹⁰⁻¹², while others have shown an influence from organic
66 matter (OM)⁸, presumably by providing complexed Fe²⁺ and/or humic electron shuttles¹³.
67 Abiotic N₂O formation has been recorded in polar^{10,14} and temperate¹¹ environments, but the
68 extent and distribution of this process in tropical peatlands have remained unexplored. With a
69 recently estimated area of 1.7 million km² (ref. ¹⁵), tropical peatlands under varying climatic
70 regimes could play a major role in global N₂O gas cycling.

71 Denitrification, generally occurring at oxygen concentrations below 6 μM¹⁶, is
72 considered to be driven predominantly by microbial communities using Fe- and Cu-dependent
73 reductase enzymes¹⁷ through a modular pathway structure with different populations mediating
74 only one or two reduction steps^{18,19}. Denitrifying microbes are well adapted to the conditions

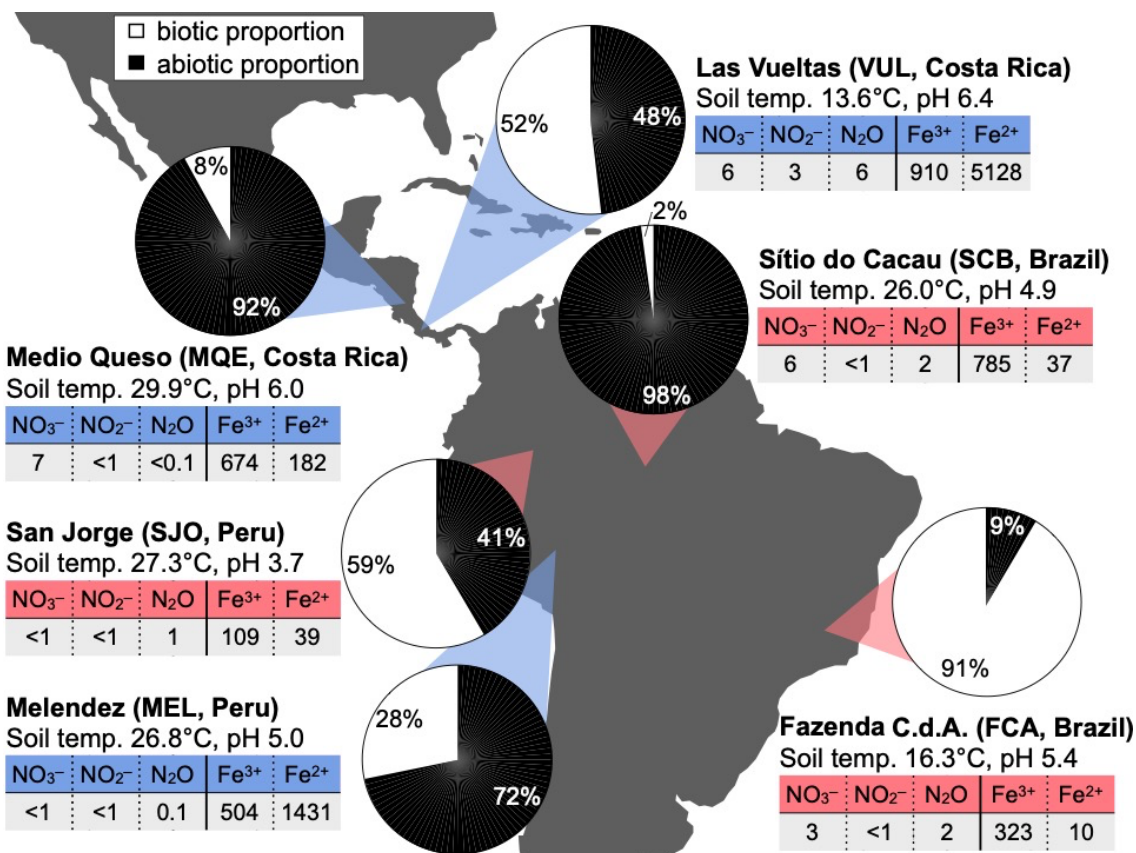
75 found in peat soils because they anaerobically respire organic substrates using nitrogen oxides
76 as terminal electron acceptors^{20,21}. Also, the extensive N₂O sink potential previously observed
77 in diverse soils^{22,23} can be better explained with the discovery of the abundant clade II N₂O-
78 reducing bacteria. While clade I N₂O-reducers are affiliated to the *Proteobacteria*, clade II N₂O
79 reducers are more diverse and scattered across multiple phyla²⁴. Interestingly, the clade II
80 members tend to lack NO₂⁻ reductases more so than clade I members²⁴. From an ecological
81 perspective, this trait might correspond with an intrinsic capability of the soil habitat to reduce
82 NO₂⁻ via chemodenitrification. Cellular resources can be saved and relocated to the expression
83 of NO and N₂O reductases²⁵ to catalyze a thermodynamically more favorable redox reaction
84 (ΔG of N₂O reduction is ~ 100 kJ mol⁻¹ higher than ΔG of NO₂⁻ reduction).

85 While interactions between microbial guilds have been proposed as the basis for
86 modularity²³, the interplay of denitrifiers with abiotic reactions has received little attention,
87 even though chemodenitrification can reduce or contribute to different inorganic nitrogen pools,
88 including N₂O and NO. The compatibility of abiotic N₂O production and modular microbial
89 denitrification led us to hypothesize that a coupled abiotic-biotic N₂O cycle could operate in
90 tropical peatlands. To test our hypothesis, we explored the dynamics and underlying factors of
91 abiotic N₂O formation and microbial N₂O reduction in six peatlands located across Central and
92 South America using isotopic tracers. Simultaneously, we quantified and sequenced the *nosZ*
93 gene as a marker for the N₂O-reducing microbial community. Our results provide evidence for
94 concomitant abiotic N₂O production and microbial consumption active under various peat soil
95 conditions.

96 **Results**

97 ***Fe²⁺ drives abiotic formation of N₂O in high-N₂O soils***

98 We assessed soil denitrification in six tropical peatlands, of which four were located
99 within or near the Amazon basin (San Jorge, SJO; Melendez, MEL; Sítio do Cacau, SCB,
100 Fazenda Córrego da Areia, FCA) and two in Central America (Medio Queso, MQE and Las
101 Vueltas, VUL) (Fig. 1). Measured steady-state concentrations of NO₂⁻ in soil pore water were
102 below detection (< 1 μM) in the majority of sites, indicating rapid cycling^{26,27}. The iron content
103 and redox balance were highly variable, with higher Fe²⁺ concentrations in mountainous peat
104 (~5 mM) and lower Fe²⁺ in oligotrophic peat (0.01-0.04 mM). To determine abiotic N₂O
105 production rates under near-natural conditions, we induced a ten-fold spike with ¹⁵NO₂⁻ *in-situ*
106 and measured ¹⁴N¹⁵NO + ¹⁵N¹⁴NO + ¹⁵N¹⁵NO evolution. Biotic activity was arrested by
107 amending the soil with 87.5 mM ZnCl₂. Because the addition of Zn can liberate Fe²⁺ ions
108 inevitably stimulating N₂O production⁸, we repeated the soil incubations in the laboratory, with
109 100 μM NO₂⁻, using both gamma-irradiated and Zn-treated peat soil. We then deduced a site-
110 specific correction factor for estimates of *in-situ* rates. All our reported abiotic N₂O production
111 rates are therefore corrected for Zn-induced N₂O production.



112
113
114
115
116
117
118
119
120

Fig. 1. Contribution of abiotic and biotic reactions to overall N₂O production in tropical peatlands. Rates were derived *in situ* from the enrichment of ¹⁵N in N₂O after addition of ¹⁵NO₂⁻ to soil in the field (n = 4). Dissolved nitrogen (measured *in-situ*) and Fe species (extracted) concentrations are given in μM. Sites are color-coded based on their NO to N₂O yield (Table 1), showing high-NO yield (red shades) or high-N₂O yield (blue shades).

121 Abiotic N₂O production was observed in all peatlands. *In-situ* rates ranged from low
122 (0.05-0.3 nmol N₂O g⁻¹ d⁻¹) at FCA and SCB, moderate (2.4-3.3 nmol N₂O g⁻¹ d⁻¹) at MQE and
123 SJO, and high (9.2-39.0 nmol N₂O g⁻¹ d⁻¹) at MEL and VUL. Abiotic N₂O production
124 contributed to the overall N₂O flux to a greater extent than biotic N₂O production at half the
125 field sites (Fig. 1). Soil Fe²⁺ concentrations measured after extraction positively correlated with
126 abiotic N₂O production rates ($R^2 = 0.99$, n = 6, Supplementary Fig. 1). To determine the
127 nitrogen yield of the chemodenitrification reaction, we incubated gamma-irradiated peat soil
128 under anoxic conditions with 100 μM NO₂⁻, and quantified NO₂⁻, NO and N₂O in time
129 (Supplementary Fig. 2). In two peatlands (SJO, SCB), complete denitrification was achieved

130 almost based purely on abiotic reactions (Table 1). The transformation of NO_2^- into NO and
131 N_2O resulted in dominant yields of either product across sites, suggesting unequal nitrogen
132 diversion directed by local peat chemistry. Our analytical approach could not confirm N_2 as a
133 byproduct²⁸, which was presumably dominant at circum-neutral pH sites (MEL and VUL). We
134 used this observed divergent NO_2^- conversion to group the diverse peat soils into high- N_2O
135 (MQE, VUL, MEL) and high-NO (FCA, SJO, SCB) abiotic-yield sites (Table 1).

136

137 To our knowledge, this study represents the first assessment of the relative contribution
138 of abiotic N_2O production to the overall N_2O production at near-natural NO_2^- levels. Based on
139 our results, abiotic reactions outcompete biotic reactions in three peatlands and are highly
140 competitive as a source of N_2O at another two. The measured N_2O production rates were
141 comparable to reported rates from a coniferous forest and grasslands²⁹, although the amount of
142 added NO_2^- was at least one order of magnitude lower in our study. Relative to other evaluated
143 ecosystems¹⁰, peat soils have less oxidized Fe or Mn minerals and are enriched in recalcitrant
144 organic carbon, which would hold additional reducing power, particularly in the structurally
145 disparate OM. For instance, pi-electron bonds are an integral part of the chemical structures
146 found in recalcitrant organic carbon, such as phenolic or humic substances, and they are prone
147 to interact with NO_2^- (refs. ^{30,31}). Besides serving as reactants, humic substances can act as
148 regenerable electron shuttles for redox reactions in soils and sediments³². Iron reduction and
149 dissolution are greatly enhanced in the presence of humic substances^{33,34}, which increases the
150 availability of Fe^{2+} . The distinct production of NO and N_2O across a gradient of Fe^{2+}
151 concentrations suggests divergent reaction mechanisms in high-NO and high- N_2O soils.
152 Previous reports agree with our data that indicate the larger production of NO as the final
153 product of chemodenitrification, which is stimulated by the self-decomposition of nitrous acid
154 in increasingly acidic soil milieu^{35,36}. High- N_2O soils coincided with high soil Fe^{2+} abundances,

155 and high-NO sites were associated with low Fe²⁺ (Fig. 1, Table 1). Besides Fe²⁺, the mixture of
156 functional groups in peat OM may also be crucial in determining the NO to N₂O balance.
157 Except for dimethyl glyoxime and quinone oximes, oxime groups preferentially produce N₂O
158 and aromatics tend to produce NO³⁷.

159 Nitrite incorporation into OM may explain lower nitrogen yields in either NO or N₂O, in
160 addition to the possible production of N₂. For example, nitrosophenol (a phenol moiety that
161 binds one NO₂⁻ ion) tautomerizes to quinone monoxime and requires another NO₂⁻ ion to eject
162 hyponitrous acid which decomposes to N₂O^{30,31}. Without the consecutive incorporation of 2
163 NO₂⁻ ions, nitrosophenol remains stable, and a significant amount of NO₂⁻ could reside in
164 nitrosated functional groups.

165

166 **Table 1. Abiotic nitrogen yield fractions based on sterilized batch incubations.** Gamma-
167 irradiated peat soil was used for anoxic incubations initiated with the addition of 100 μM NO₂⁻.
168 Yield was calculated after all NO₂⁻ was consumed and based on stable NO and N₂O
169 concentrations in at least two consecutive measurements. Sites with replicated samples (n = 3)
170 included: Las Vueltas (VUL), Medio Queso (MQE), Fazenda Córrego da Areia (FCA),
171 Melendez (MEL), Sítio do Cacau (SCB), San Jorge (SJO).

	SCB	SJO	FCA	MEL	VUL	MQE
Yield in NO (%)	97.2	92.8	74.3	0.2	0.2	1.3
Yield in N ₂ O (%)	4.8	4.8	4.0	12.1	24.6	55.9
Total yield (%)	102	97.6	78.3	12.3	24.8	57.2

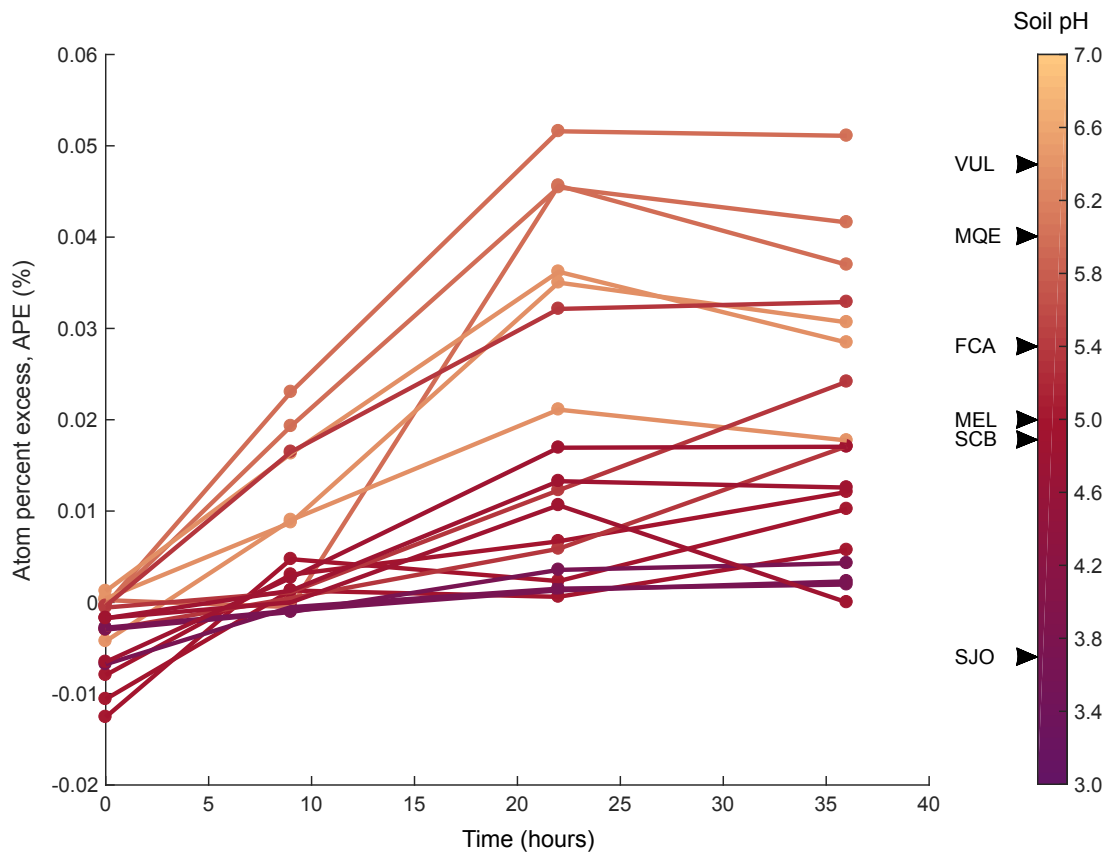
172

173

174 *Active microbial N₂O reduction in acidic peat soils*

175 Concomitant to N₂O production, we measured N₂O consumption. Only non-sterilized
176 samples exhibited active consumption. In sterilized samples, N₂O was a stable end product after
177 NO₂⁻ addition, and ¹⁵N₂ was not produced in (¹⁵N)₂O amendments. Incubations with (¹⁵N)₂O in
178 the field resulted in an accumulation of the ¹⁵N label in N₂ (Fig. 2) and were used to derive N₂O
179 reduction rates. Enrichment of ¹⁵N₂ decreased with soil pH (Fig. 2), while N₂O reduction was

180 surprisingly observed in soils with pH as low as 3.7 (SJO). This finding is significant because
181 N₂O reductase assembly is post-transcriptionally inhibited by acidic pH³⁸, and exposure to pH <
182 4 disrupts a histidine amino acid ligand to the Cu cofactor in N₂O reductase, possibly
183 inactivating the catalytic function (pers. com. W. Nitschke). The measured N₂O reduction rates
184 were higher than previously observed rates at similar acidic pH values³⁹ and would extend the
185 known physiological limits for microbial N₂O consumption. Thus, these results demonstrate the
186 presence and activity of N₂O-reducing communities adapted to a wide range of peat soil pH.



187

188 **Fig. 2. Isotopic enrichment in molecular nitrogen during *in-situ* incubations of (¹⁵N)₂O**
189 **with anoxic peat soil.** Replicates per sites (n = 3), as listed, are colored in a gradient according
190 to their pH. VUL, Las Vuelas; MQE, Medio Queso; FCA, Fazenda Córrego da Areia; MEL,
191 Melendez; SCB, Sítio do Cacau; SJO, San Jorge.

192

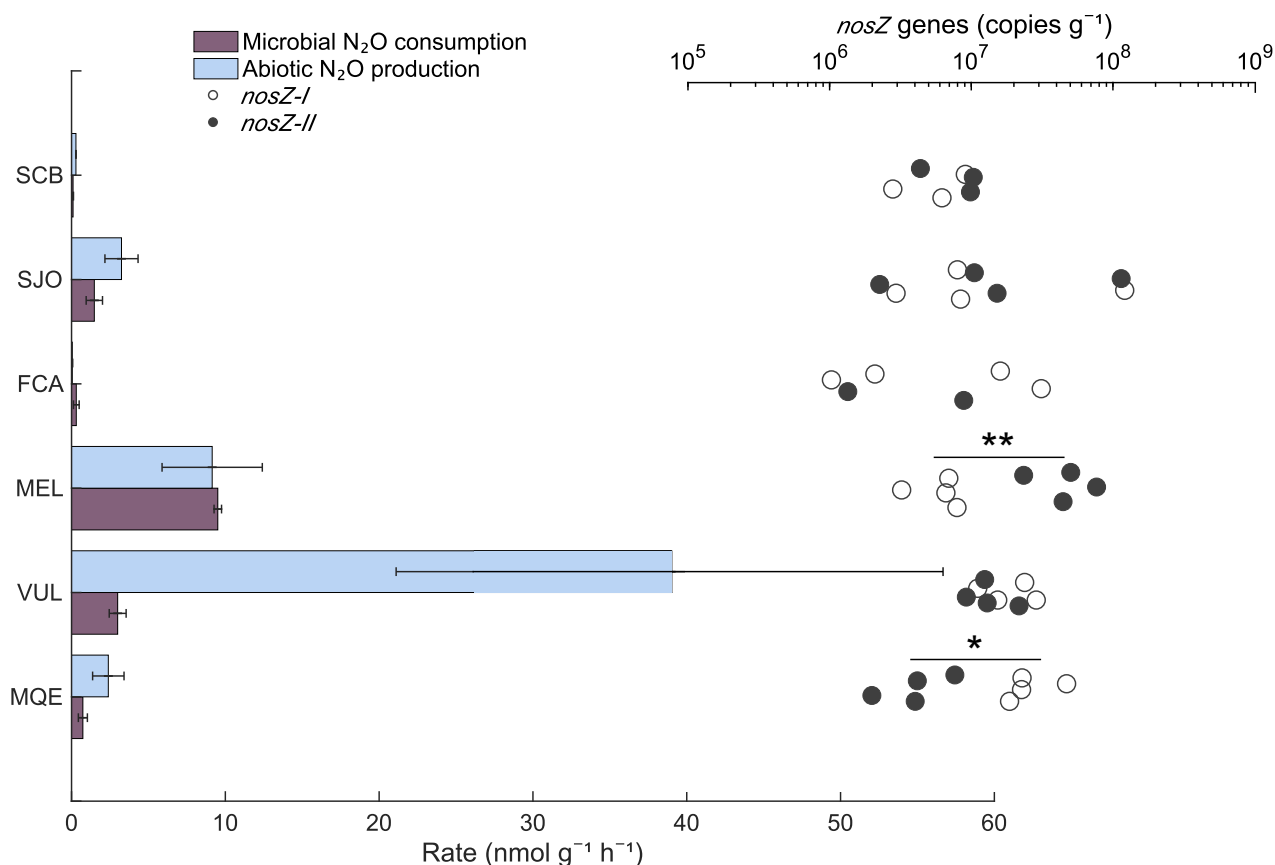
193

194

195

196 ***Diverse Clade II N₂O-reducers are associated with higher N₂O sink potential***

197 To evaluate the relationship between the abiotic formation and microbial consumption
198 of N₂O, we compared reaction rates against *nosZ* gene abundances. Both processes revealed
199 similar trends ranging from low (0.1-0.3 nmol N₂O g⁻¹ d⁻¹) in SCB and FCA to moderate (0.7-
200 1.5 nmol N₂O g⁻¹ d⁻¹) in MQE and SJO to high (3-9.5 nmol N₂O g⁻¹ d⁻¹) in VUL and MEL.
201 Consumption never outpaced production, except at two sites (FCA and MEL, Fig. 3). While the
202 variation in *nosZ* gene copies from both clades showed no significant differences among high-
203 NO sites (FCA, SJO, SCB), they differed (ANOVA, *p* = 0.05) among high-N₂O sites (MQE,
204 MEL). Consumption rates gradually increased with clade II *nosZ* gene abundance at high-N₂O
205 sites. A clear dominance of clade II *nosZ* genes over those from clade I coincided with the
206 elevated rates of N₂O consumption in MEL peatland. Thus, N₂O reducers from clade II
207 establish an increased microbial N₂O sink in peatlands with high abiotic N₂O fluxes.



208

209 **Fig. 3. Microbial N₂O consumption and abiotic N₂O production (bars) along with *nosZ***
210 **gene quantities (open and filled circles).** Error bars denote SD (consumption rates, n = 3;
211 production rates, n = 4). Clade I and II *nosZ* was quantified by qPCR assays and are
212 significantly different within sites as denoted by asterisks (ANOVA, **p* = 0.012, ***p* = 0.008, n
213 = 4). Two outliers for *nosZ-II* (SCB, ~6,200 copies g⁻¹; FCA, ~590) are not shown and another
214 two datapoints are missing due to non-amplification. See previous figures for site acronyms.
215

216 Next, to evaluate the N₂O-reducing microbial community, we analyzed 183,265 and
217 80,050 taxonomically assigned *nosZ* gene amplicon sequence variants (ASVs) for clade I and
218 II, respectively. Our analysis focused on the most abundant taxa that made up at least 1% of the
219 total ASVs in at least one site (Fig. 4). The most abundant ASV was affiliated to the alpha-
220 proteobacterium *Nitrospirillum amazonense* (Fig. 4). This phylotype constituted 59-64 % of
221 clade I ASVs in the Amazon bogs SCB and SJO but was least represented in the MEL peatland
222 (~10 %). In MEL, 23 % of ASVs belonged to *Methylocystis* species, which were also abundant
223 in FCA (27 %). The clade II N₂O reducers were more diverse (comprised more phyla) across all
224 soils (Fig. 4), with *Magnetospirillum* (consistently > 10 % in high-NO sites and 30 % in VUL)
225 and unclassified *Myxococcales* (8-50 %) as the most abundant phylotypes. To examine the
226 observed trend of N₂O reduction rates corresponding with *nosZ* clade II gene frequencies in the
227 high-N₂O sites (MEL > VUL > MQE, Fig. 3), we derived diversity indices and performed a
228 principal component analysis (PCA). The Shannon diversity index showed a coinciding order of
229 diversity levels (1.73 > 1.49 > 1.39, Supplementary Tables 1a-b) for high-N₂O sites. This was
230 also supported by a relatively high average Bray-Curtis dissimilarity of clade II *nosZ* gene
231 sequences in MEL (0.71, Supplementary Tables 1c-d), identifying the clade II N₂O reducer
232 community in this peatland as most dissimilar to all others. In addition, the community structure
233 variation among clade II was most parsimoniously explained by N₂O consumption rates in the
234 PCA (Supplementary Figs. 3, 4). Rather than single dominant taxa, it appeared to be the
235 contribution of a diverse group of clade II N₂O reducers to be responsible for the high N₂O sink
236 potential observed.

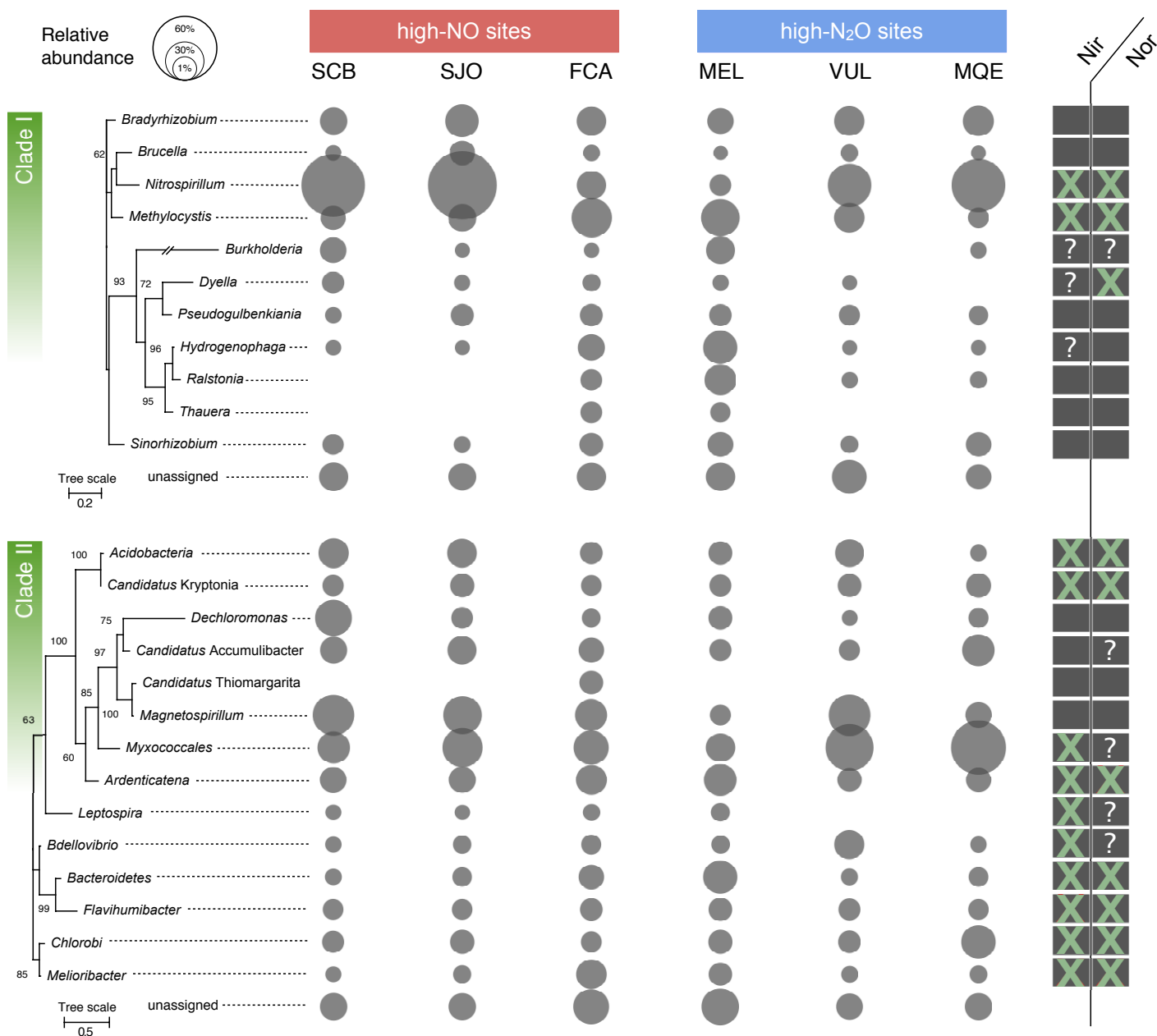
237 The intrinsic capacity of the peat to reduce NO_2^- abiotically could provide non-
238 denitrifying microbes that do not possess denitrification enzymes other than N_2O reductase,
239 called “chemodenitrifiers”⁴⁰, an advantage over canonical denitrifiers. Chemodenitrifiers do not
240 have to compete with chemodenitrification and simply harvest the end product N_2O to oxidize
241 organic substrates. Figure 4 illustrates the NO_2^- reductase (either NirS or NirK) and NO
242 reductase (NorB) enzyme repertoires present in available reference proteomes of relatives of the
243 predicted taxa in both clades. At least 2 out of the 11 clade I taxa (including the abundant
244 *Nitrospirillum*) and 10 out of the 14 clade II taxa indicated the absence of Nir enzymes (Fig. 4).
245 Half of the clade II reference proteomes were missing both Nir and Nor proteins. Importantly,
246 the Myxococcales ASVs showed no differences in abundance among high-NO sites but
247 gradually increased, similar to the N_2O yield, in the high- N_2O sites. This order, which also
248 includes *Anaeromyxobacter dehalogenans*, the hallmark organism of clade II N_2O reducers^{22,41},
249 is frequently represented in acidic, organic-rich soils^{40,42}, presumably with abiotic NO and N_2O
250 production potential. Further, other bacteria such as *Dechloromonas*⁴³, *Ardenticatena*⁴⁴, and
251 *Melioribacter*⁴⁵ also mediate iron reduction, an additional trait that could promote
252 chemodenitrification by recycling Fe^{2+} . Therefore, chemodenitrifiers may outcompete canonical
253 denitrifiers in the studied peatlands (e.g., *Nitrospirillum*) and abundance patterns of the
254 Myxococcales suggest a notable benefit for some chemodenitrifiers in soils associated with
255 high abiotic N_2O yields.

256 Another abundant taxon of the N_2O -reducing community was *Magnetospirillum* (clade
257 II) that includes several iron-oxidizing species. These alpha-proteobacteria synthesize the
258 mixed-valence iron mineral magnetite, which can accumulate in soils, also under the influence
259 of abiotic crystallization⁴⁶. Secondary iron mineral formation can be widespread in the tropics,
260 driven by dissolved and particulate iron originating from weathering and desilication⁴⁷⁻⁴⁹.
261 Ferrous iron-bearing minerals, such as magnetite, can serve as catalysts for NO_2^- reduction by

262 providing reaction sites at the mineral surface^{50,51}. The possession of an N₂O reductase makes
 263 sense for *Magnetospirillum*, assuming cells are associated with, or at least grow in proximity to,
 264 magnetite. Analyses of the iron phases present would be necessary to follow up on this in more
 265 detail, which was off the scope of our study. We also acknowledge that our insight into the
 266 temporal activity response is limited. Information on the actual *in-situ* transcription levels is
 267 needed to better assess how the clades react to fluctuating abiotic pulses of N₂O⁵².

268

269



270

271 **Fig. 4. NosZ phylogeny and taxonomy in tropical peat soils.** Only the most abundant
272 amplicon sequence variants (ASVs) > 1 % were included in the analysis. Maximum likelihood
273 phylogenetic trees are based on 1000 iterations. Nodes with 60 % or higher bootstrap support
274 are labeled. The right panel indicates the presence (filled box) or absence (crossed box) of Nir
275 or Nor enzyme sequences in reference proteomes. Boxes with question marks indicate an
276 ambiguous distribution of Nir or Nor within the taxonomic group (Supplementary Table 2).

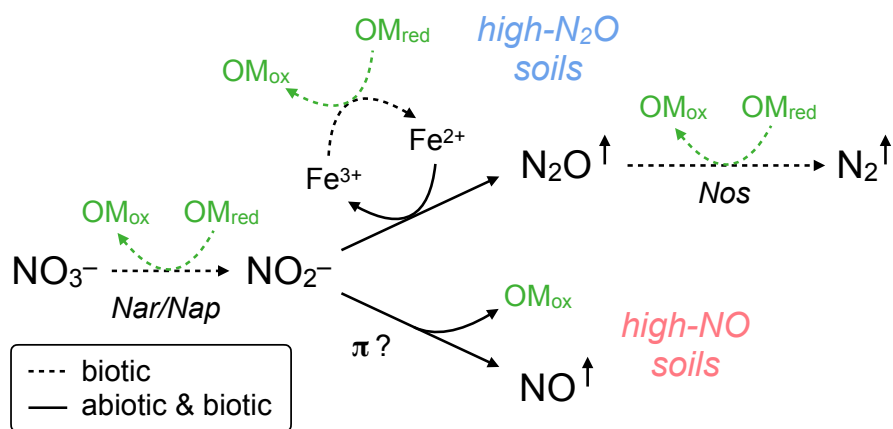
277 **Discussion**

278 ***Decoupling of abiotic N₂O production and microbial N₂O consumption***

279 Our data show the concomitant occurrence of both abiotic N₂O production and
280 microbial consumption (Fig. 3 and Supplementary Fig. 2), and their positive correlation points
281 to the coupling of both processes in several sites (Supplementary Fig. 5). However, the
282 mountain bog site (VUL) exhibited unusually high abiotic production rates and relatively low
283 consumption rates (Fig. 3). A lower soil temperature than in the other peatlands and the
284 differential sensitivity of production and consumption (Supplementary Table 3 and
285 Supplementary Text) could lead to such kinetic effects⁵³⁻⁵⁵. Along these lines, the decoupling of
286 production and consumption establishes the potential for vast N₂O emissions when changing
287 environmental conditions impart selectively negative effects on consumption. For instance,
288 while peatland drainage occurs naturally between wet and dry seasons⁵⁶, N₂O cycling could
289 become decoupled by aerobic conditions created by extended peatland drainage with microbial
290 denitrification persisting only in anoxic microsites. Nitrite, fueled by increased nitrification,
291 could still be abiotically reduced to N₂O because acidic peat soil stabilizes Fe²⁺ via two
292 mechanisms. First, Fe²⁺ oxidation by oxygen is kinetically hindered at low pH. Oxidation rates
293 are significantly slowed at pH ≤ 6.5⁵⁷, a pH regime applying to most peatlands, including all in
294 our study. Second, Fe²⁺ complexed by OM is resilient to oxidation. Experimental evidence
295 suggests that tannic acid⁵⁸, phenolics⁵⁹, or natural humic acid⁶⁰ stabilize the Fe²⁺ pool in the
296 presence of oxygen by the formation of a redox-buffering shell⁶⁰ and re-reduction of Fe³⁺.
297 However, little is known concerning how Fe²⁺ complexation affects the NO₂⁻ accessibility and
298 reduction. Nevertheless, these previous findings indicate that the reactants for
299 chemodenitrification are sufficiently available even at higher oxygen concentrations (> 6 μM),
300 leading to a potential predominance of abiotic N₂O production over biotic N₂O production.

301

302



303 **Fig. 5. Schematic representation of denitrification pathways in tropical peatlands.** Nitrate
 304 (NO_3^-) reduction to NO_2^- occurs at significant rates only with catalysis by NO_3^- reductases.
 305 Nitrite is rapidly reduced via abiotic and biotic reactions. At lower pH (≤ 5.4), NO is the
 306 dominant product. Nitrosation into OM may be an alternative abiotic process in soils with
 307 minor nitrogenous gas production reliant on organic compounds containing pi-electron bonds
 308 (π). In Fe^{2+} -rich peat, N_2O is the dominant product, involving Fe redox cycling that can fuel
 309 dissimilatory Fe reduction¹¹. The only N_2O consumption pathway in peat soil is N_2O reductase-
 310 dependent reduction to N_2 , which is active even in the most acidic soils tested (pH 3.7). All
 311 related heterotrophic reactions induce oxidation of OM ($\text{OM}_{\text{red}} \rightarrow \text{OM}_{\text{ox}}$) and eventually peat
 312 carbon mineralization.

313

314 We present evidence that active abiotic-biotic N_2O cycling is prevalent in tropical
 315 peatlands, where denitrification is not a purely biological pathway, but rather a “mosaic” of
 316 biotic and abiotic reduction reactions (Fig. 5). Furthermore, our results support the idea that
 317 functional modularity complements not only the interrelationship of microbial groups but also
 318 concomitant interactions between microbes and spontaneous chemical reactions. Abiotic N_2O
 319 formation in tropical peatlands can have important regional consequences in the context of
 320 observed N_2O fluxes and higher rates in response to drainage⁶¹, and putatively drought⁶², as
 321 well as possible effects on reducing organic carbon release⁶³. For example, compared to the
 322 other soils, abiotic N_2O production was moderate in SJO, an acidic oligotrophic site, showing a
 323 net production of $1.8 \text{ nmol } \text{N}_2\text{O } \text{g}^{-1} \text{ day}^{-1}$. With the estimation of the global extent of acidic
 324 oligotrophic tropical peatlands alike SJO at $1,003,719 \text{ km}^2$ (ref. 15), this could amount to a total
 325 depth-integrated abiotic N_2O flux ranging from 0.1 to $3.9 \text{ Tg } \text{N}_2\text{O } \text{yr}^{-1}$ depending on the depth
 326 of NO_2^- diffusion. This contribution is a major uncertainty that could account for two percent to

327 more than half of all combined terrestrial N₂O fluxes from natural sources of South America,
328 Africa, and Southeast Asia. With a factor of 298 g CO₂-equivalents per g N₂O over a 100 year
329 time⁶⁴, abiotic N₂O fluxes could also alter the net radiative effect of tropical peatlands.
330 Accordingly, by bypassing heterotrophic respiration through chemodenitrification, less organic
331 carbon is mineralized to CO₂. Considering ~50 mg CO₂-C m⁻² yr⁻¹ emitted from SJO-like
332 tropical peatlands⁷ and 4 moles of N₂O required to mineralize 1 mole of organic carbon,
333 chemodenitrification would suppress at least 2.7 % of the organic carbon mineralization,
334 promoting the retention of 2 Tg C yr⁻¹ across oligotrophic tropical peatlands. These estimates
335 are conservative because they do not include processes such as diversion of nitrogen oxides into
336 NO, nitrosation of OM, and the consumption deficit observed in the high-altitude peatland.
337 Sensitivity to lower temperatures could also impede microbial N₂O reduction in northern
338 peatlands, which would imply an imbalanced cycling of N₂O and substantial N₂O release from
339 abiotic origins.

340 **Methods**

341

342 **Study sites.** Six peatlands were chosen to cover a geochemical spectrum, including acidic (pH
343 3.7-5) soils, low (10 μM) and high ($> 5 \text{ mM}$) Fe^{2+} concentrations, varying OM content and soil
344 temperature (Supplementary Table 4). Most sites were under little to no anthropogenic
345 influence (Supplementary Table 5), with two exceptions: Fazenda Córrego da Areia (FCA)
346 located within a catchment experiencing agricultural run-off in Brazil, and Medio Queso
347 (MQE) in a Costa Rican river delta surrounded by agricultural run-off and cattle raising. The
348 San Jorge (SJO) peatland is located in the Pastaza-Marañón foreland basin and Melendez
349 (MEL) is in the Madre de Dios river terraces, both in Peru. Sítio do Cacau (SCB) is located in
350 Central Amazonia (Amanã Reserve) in Brazil. Las Vueltas (VUL), located in Costa Rica's
351 cloud forests of the Cerro Las Vueltas Reserve, differed most drastically from the other sites
352 due to its higher altitude (2,500 m a.s.l.). Field work was conducted in September 2017 (Peru)
353 and between April (Costa Rica) and July (Brazil) in 2018.

354

355 ***¹⁵N tracer experiment in the field.*** Colorimetric assays to determine ambient soil NO_2^- and
356 NO_3^- concentrations were performed in the field using a YSI 9500 portable spectrophotometer
357 (YSI Inc.), including reagent kits, according to the manufacturer's instructions. Dissolved N_2O
358 was sampled by collecting pore water into a pre-evacuated vial and subsequent degassing by
359 shaking for 5 minutes. Thereafter, headspace was transferred into a pre-evacuated vial and
360 stored underwater prior to analysis with a GC-ECD. Soil temperature and pH were measured
361 with a YSI A10 pH probe (Ecosense, YSI).

362 Anaerobic glove bags filled with argon (Ar) were used to provide anaerobic conditions
363 in the field while distributing soil into glass incubation vials (160 mL). Topsoils (10 cm) were
364 sampled with 30 ml-barrel customized plastic corers. Inside the glove bag, the center 5 cm (~ 15
365 g) soil was diluted 1:5 (w/v) into vials with anoxic water extracted directly from the deep peat

366 soil via a water line connected to the glove bag. Separate sample sets received $^{15}\text{NO}_2^-$ (label
367 fraction = 0.1, Cambridge Isotopes) at $10\times$ the soil ambient NO_2^- concentration and doubly
368 labeled $(^{15}\text{N})_2\text{O}$ (label fraction = 1.0, Cambridge Isotopes) at $5\times$ the soil ambient N_2O
369 concentration. Thus, the amount of ^{15}N tracer applied varied slightly between sites but reflected
370 a similar order of magnitude. $^{15}\text{NO}_2^-$ incubations included untreated and 87.5 mM zinc chloride-
371 poisoned (ZnCl_2 , Fisher Scientific) soils in replicates of four ($n = 4$). Soil slurries were
372 incubated in insulating containers to avoid temperature fluctuations, and gas samples were
373 taken for $(^{15}\text{N})_2\text{O}$ analysis at the beginning of incubation and after 24 h ($n = 4$), and for $^{30}\text{N}_2$
374 analysis at four time points spread over 36 h ($n = 3$). Gas sampling was destructive (entire
375 headspace used) for $(^{15}\text{N})_2\text{O}$ analysis or by replacement with 5 mL Ar gas for $^{30}\text{N}_2$ analysis. The
376 sample times for the $^{30}\text{N}_2$ analysis were adapted from a previous study⁶⁵. We also prepared zinc-
377 poisoned $(^{15}\text{N})_2\text{O}$ incubations to test for abiotic N_2O consumption. The gas samples were stored
378 underwater in borosilicate glass vials closed with thick butyl rubber stoppers⁶⁶ prior to analysis
379 at Michigan State University. Isotopic compositions of N_2O and N_2 were measured using an
380 Elementar Isoprime isotope ratio mass spectrometer (IR-MS) interfaced with an Elementar
381 TraceGas chromatographic system. Rate calculations closely followed a previously developed
382 and tested protocol¹⁴. Given the constraints of sterilant applications in the field, we repeated the
383 zinc-amended incubations in the lab, complementarily to incubations with gamma-irradiated
384 soils. The rates from both experiments were used to calculate a correction factor accounting for
385 artifacts caused by the zinc addition⁸. The rates derived in the field were then multiplied by the
386 correction factor (Supplementary Fig. 6 and Supplementary Table 6). The Brazilian sites SCB
387 and FCA have associated data from gamma-irradiated soil, but data from zinc-treated soil are
388 missing because of logistic issues concerning the shipment of non-sterilized (not gamma-
389 irradiated) soil. The final rates were combined according to the following equation for net *in-*
390 *situ* N_2O formation:

391
$$B = M + C - A$$

392 where B is the biotic N_2O production rate, M is the mixed rate (from untreated $^{15}\text{NO}_2^-$
393 incubations), C is the microbial N_2O consumption rate [from $(^{15}\text{N})_2\text{O}$ incubations], and A is the
394 abiotic N_2O production rate (from poisoned $^{15}\text{NO}_2^-$ incubations).

395
396 **Laboratory incubations.** In an anoxic glove box (0.1% H_2 for O_2 reduction in N_2), gamma-
397 sterilized and zinc-treated soil were prepared separately. Gamma sterilization followed a
398 previous method⁸. Zinc chloride was applied, as described for field experiments. Roots and
399 coarse particles (> 5 mm in diameter) were removed from soils, and soils were slurried 1:5
400 (w/v) in anoxic, sterile 18.2 M Ω -cm water. The slurry was homogenized before equal quantities
401 were distributed into culture vials and sealed with sterile butyl rubber stoppers. An anoxic and
402 filter-sterilized NO_2^- solution was injected (final concentration 100 μM) into microcosms that
403 were previously flushed with pure N_2 . The microcosms were agitated briefly to disperse the
404 added substrate and then kept under dark, static conditions at room temperature for ~100 h.
405 Dissolved NO_2^- was quantified with the Griess reagent (Promega, Kit G2930), and NO and
406 N_2O were analyzed as described below.

407
408 **Soil Fe measurements.** Soils for Fe analysis were kept in anoxic serum bottles and refrigerated
409 during transport. The species Fe^{2+} and Fe^{3+} were extracted and separated as previously
410 described⁸ and quantified in acidified aqueous solution by inductively coupled plasma–optical
411 emission spectrometry (ICP-OES; Thermo iCAP6300 at the Goldwater Environmental
412 Laboratory at Arizona State University). The ICP-OES pump rate for the Ar carrier was set to
413 50 rpm, and Fe2395 and Fe2599 lines were used for Fe quantification. Iron concentrations were
414 determined from a calibration curve (0.01-10 mg L^{-1}) by diluting a standard solution (100 mg
415 L^{-1} , VHG Labs, product no. SM75B-500) in 0.02 N HNO_3 .

416

417 ***N₂O gas measurements.*** Using a gas-tight syringe (VICI Precision Sampling), 200 μ L of gas
418 sample was injected into a gas chromatograph (GC, SRI Instruments) equipped with an
419 electron-capture detector (ECD). Two continuous HayeSep-D columns were kept at 90 °C
420 (oven temperature), and N₂ (UHP grade 99.999 %, Praxair Inc.) was used as carrier gas. The
421 ECD current was 250 mV, and the ECD cell was kept at 350 °C. The N₂O measurements were
422 calibrated over a range of 0.25-100 ppmv using customized standard mixtures (Scott Specialty
423 Gases, accuracy ± 5 %). Gas concentrations were corrected for solubility effects using Henry's
424 law and the dimensionless concentration constant $k_H^{cc}(\text{N}_2\text{O}) = 0.6112$ to account for gas
425 partitioning into the aqueous phase at 25 °C and 1 atm⁶⁷.

426

427 ***NO gas measurements.*** Nitric oxide (NO) was quantified in the microcosm headspace with a
428 chemiluminescence-based analyzer (LMA-3D NO₂ analyzer, Unisearch Associates Inc.,
429 Concord, Canada). Headspace gas (50 μ L) was withdrawn with a CO₂-N₂-flushed gas-tight
430 syringe and injected into the analyzer. The injection port was customized to fit the injection
431 volume and consisted of a T-junction with an air filter at one end and a septum at the other end.
432 An internal pump generated consistent airflow. Our method followed a previous protocol⁶⁸,
433 with minor adjustments. Briefly, NO was oxidized to NO₂ by a CrO₃ catalyst. The NO₂ was
434 carried across a fabric wick saturated with a Luminol solution (Drummond Technology Inc.,
435 Canada). Readings were corrected for background NO₂ every 15 min ("zeroing"). Shell airflow
436 rate was kept at 500 mL min⁻¹, and the span potentiometer was set to 8. Measurements were
437 calibrated with a 0.1 ppm NO (in N₂) standard (< 0.0005 ppm NO₂, Scott-Marlin, Riverside,
438 CA, USA) over a range of 5-1,000 ppbv. Gas concentrations were corrected using Henry's law
439 and the dimensionless concentration constant $k_H^{cc}(\text{NO}) = 0.0465$ to account for gas partitioning
440 into the aqueous phase at 25 °C and 1 atm⁶⁷.

441

442 ***Molecular analyses.*** Peat samples from four randomly distributed locations (coinciding with
443 incubation locations) within a peatland were collected and frozen at $-20\text{ }^{\circ}\text{C}$ for subsequent
444 DNA extraction. Genomic DNA was extracted using a NucleoSpin Soil DNA extraction kit
445 (Macherey-Nagel GmbH, Düren, Germany).

446 For quantitative polymerase chain reactions (qPCR), we used two primer pairs and a
447 total reaction volume of $15\text{ }\mu\text{L}$ with $1.5\text{ }\mu\text{L}$ DNA template (35-50 ng genomic DNA). The clade
448 I *nosZ* gene was amplified with PowerUp SYBR Green master mix (Applied Biosystems,
449 Foster City, CA), to which 3 mM MgCl_2 was added. Forward and reverse primer concentrations
450 were $1\text{ }\mu\text{M}$, and previous cyclor conditions were used⁶⁹. The clade II *nosZ* gene was amplified
451 using SYBR Fast, ROX low master mix (Kapa Biosystems, Roche Holding AG, Basel,
452 Switzerland), and $1.2\text{ }\mu\text{M}$ primer concentration⁷⁰. Thermal cycling was initiated with 3 min of
453 denaturing at $95\text{ }^{\circ}\text{C}$, followed by 40 cycles of the following stages: 30 s at $95\text{ }^{\circ}\text{C}$, 60 s at $58\text{ }^{\circ}\text{C}$,
454 30 s at $72\text{ }^{\circ}\text{C}$, 30 s at $80\text{ }^{\circ}\text{C}$, and a final melting-curve. Samples were run in technical duplicates
455 on 96-well plates using a Quantstudio 3 thermocycler (Applied Biosystems, Foster City, CA).
456 Standards were prepared using linearized plasmids. Standard curves indicated efficiencies of 94
457 % ($R^2 = 0.99$, *nosZ* clade I) and 85 % ($R^2 = 0.99$, *nosZ* clade II) and melting curves showed no
458 detectable primer dimers over the duration of 40 amplification cycles.

459 For Illumina amplicon sequence analysis, we developed independent *nosZ* clade I and II
460 libraries. PCR-amplification of both *nosZ* genes used the Promega GoTaq qPCR kit (Promega,
461 Madison, WI) and $1\text{ }\mu\text{L}$ of DNA template (25-50 ng genomic DNA) in a total reaction volume
462 of $20\text{ }\mu\text{L}$. Targeting the clade I *nosZ* gene, we used a novel primer pair⁷¹. The reaction mix
463 included 0.2 mg mL^{-1} bovine serum albumin (BSA) and $0.8\text{ }\mu\text{M}$ primer concentration. For the
464 clade II *nosZ* gene, we used the same primer as used for qPCR in reactions of 1 mg mL^{-1} BSA
465 and $0.8\text{ }\mu\text{M}$ primer concentration. Cycling conditions for clade II *nosZ* amplification were used

466 as described⁷⁰. Thermal cycling conditions for clade I *nosZ* amplification were an initial 2 min
467 denaturing step at 95 °C, followed by 33 cycles of 95 °C for 45 s, annealing by 53 °C for 45 s,
468 and a 72 °C extension for 30 s, and a final extension at 72 °C for 7 min. Amplification was
469 verified by gel electrophoresis using 1 % agarose in 1 Tris-acetate-EDTA buffer. Samples were
470 multiplexed⁷², normalized (SequalPrep kit #1051001, Invitrogen), and submitted for sequencing
471 to the DNASU core facility at Arizona State University, with 2× 300-bp paired-end Illumina
472 MiSeq.

473 Paired-end sequences were merged and demultiplexed, then we used the USEARCH
474 pipeline⁷³ to 1) correct strand orientations, 2) sort out singletons, and 3) denoise the dataset. We
475 used $\alpha = 2$ for a stringent denoising of sequences⁷⁴ because reads were not clustered with
476 any identity radius to obtain ASVs. The sequences were translated and frameshift-corrected by
477 Framebot⁷⁵ with low sequence loss (< 10 %). The amino acid sequences obtained were
478 classified using Diamond⁷⁶ version 0.9.25. The search was conducted in Diamond's *sensitive*
479 mode, with an e-value cutoff of 10^{-5} , resulting in the top 5 % hits. Sequences were parsed
480 through two databases; the NCBI database RefSeq (release 95) containing 146,381,777 non-
481 redundant protein sequences and manually curated databases built from 2,817 (clade I) and
482 2,929 (clade II) sequences off the FunGene repository⁷⁷ using the search parameters 80 %
483 HMM coverage and a minimum length of 550 amino acids. The taxonomy achieved with the
484 curated databases was used for downstream analysis because of a higher number of classified
485 sequences. The output was imported into Megan⁷⁸ version 6.18.0, where a weighted lowest
486 common ancestor (LCA) algorithm [default parameters according to Huson et al.⁷⁹] was run to
487 assign a single taxonomic lineage to each read. ASV tables were pasted into Krona⁸⁰ for visual
488 inspection of results. Reads with abundances of > 1 % in at least one site were extracted, and
489 consensus sequences were determined for each taxonomic group. Maximum-likelihood
490 phylogenetic trees were constructed with consensus sequences in Mega X⁸¹. To infer

491 presence/absence of Nir and Nor enzymes in representative proteomes, UniProt reference
492 (manually curated) proteomes were screened using BlastP with default parameters. NirS
493 (Q51700, *Paracoccus denitrificans* PD1222), NirK (O31380, *Bradyrhizobium japonicum*),
494 NorB (Q51663, *Paracoccus denitrificans*) were used as amino acid query sequences.

495 The *nosZ* sequences have been deposited in the GenBank, EMBL, and DDBJ databases
496 as SRA Bioproject XXX.

497

498 ***Statistical analyses.*** All statistical tests were performed with JMP Pro software (Version 13.1.0,
499 SAS Institute Inc.). Analysis of variance (ANOVA) was used with $p < 0.05$ to test significantly
500 different values for gene quantities across soils. Plotting and regression analysis were done with
501 the Matlab R2018a software package (Version 9.4.0.813654, Mathworks Inc.).

502 **References**

503

- 504 1. Thompson, R. L. *et al.* Acceleration of global N₂O emissions seen from two decades of
505 atmospheric inversion. *Nat. Clim. Change* **9**, 993–998 (2019).
- 506 2. Tian, H. *et al.* A comprehensive quantification of global nitrous oxide sources and sinks.
507 *Nature* **586**, 248–256 (2020).
- 508 3. Zhuang, Q., Lu, Y. & Chen, M. An inventory of global N₂O emissions from the soils of
509 natural terrestrial ecosystems. *Atm. Environ.* **47**, 66–75 (2012).
- 510 4. Huang, J. *et al.* Estimation of regional emissions of nitrous oxide from 1997 to 2005
511 using multinetwork measurements, a chemical transport model, and an inverse method. *J.*
512 *Geophys. Res.* **113**, 197–19 (2008).
- 513 5. D'Amelio, M. T. S., Gatti, L. V., Miller, J. B. & Tans, P. Regional N₂O fluxes in
514 Amazonia derived from aircraft vertical profiles. *Atmos. Chem. Phys.* **9**, 8785–8797
515 (2009).
- 516 6. Teh, Y. A., Murphy, W. A., Berrío, J.-C., Boom, A. & Page, S. E. Seasonal variability in
517 methane and nitrous oxide fluxes from tropical peatlands in the western Amazon basin.
518 *Biogeosciences* **14**, 3669–3683 (2017).
- 519 7. Finn, D. R. *et al.* Methanogens and methanotrophs show nutrient-dependent community
520 assemblage patterns across tropical peatlands of the Pastaza-Marañón basin, Peruvian
521 Amazonia. *Front. Microbiol.* **11**, (2020).
- 522 8. Buessecker, S. *et al.* Effects of sterilization techniques on chemodenitrification and N₂O
523 production in tropical peat soil microcosms. *Biogeosciences* **16**, 4601–4612 (2019).
- 524 9. Heil, J., Liu, S., Vereecken, H. & Brüggemann, N. Abiotic nitrous oxide production from
525 hydroxylamine in soils and their dependence on soil properties. *Soil Biol. Biochem.* **84**,
526 107–115 (2015).
- 527 10. Samarkin, V. A. *et al.* Abiotic nitrous oxide emission from the hypersaline Don Juan
528 Pond in Antarctica. *Nat. Geosci.* **3**, 341–344 (2010).
- 529 11. Otte, J. M. *et al.* N₂O formation by nitrite-induced (chemo)denitrification in coastal
530 marine sediment. *Sci. Rep.* **9**, 1–12 (2019).
- 531 12. Jones, L. C., Peters, B., Pacheco, J. S. L., Casciotti, K. L. & Fendorf, S. Stable isotopes
532 and iron oxide mineral products as markers of chemodenitrification. *Environ. Sci.*
533 *Technol.* **49**, 3444–3452 (2015).
- 534 13. Stevenson, F. J. & Swaby, R. J. Nitrosation of soil organic matter: I. Nature of gases
535 evolved during nitrous acid treatment of lignins and humic substances. *Soil Sci. Soc. Am.*
536 *J.* **28**, 773–778 (1964).
- 537 14. Ostrom, N. E., Gandhi, H., Trubl, G. & Murray, A. E. Chemodenitrification in the
538 cryoecosystem of Lake Vida, Victoria Valley, Antarctica. *Geobiology* **14**, 575–587
539 (2016).
- 540 15. Gumbrecht, T. *et al.* An expert system model for mapping tropical wetlands and
541 peatlands reveals South America as the largest contributor. *Glob. Change Biol.* **23**, 3581–
542 3599 (2017).
- 543 16. Seitzinger, S. *et al.* Denitrification across landscapes and waterscapes: A synthesis. *Ecol.*
544 *Appl.* **16**, 2064–2090 (2006).
- 545 17. Glass, J. B. & Orphan, V. J. Trace metal requirements for microbial enzymes involved in
546 the production and consumption of methane and nitrous oxide. *Front. Microbiol.* **3**, 1–20
547 (2012).
- 548 18. Graf, D. R. H., Jones, C. M. & Hallin, S. Intergenomic comparisons highlight modularity
549 of the denitrification pathway and underpin the importance of community structure for
550 N₂O emissions. *PLoS ONE* **9**, e114118 (2014).

- 551 19. Roco, C. A., Bergaust, L. L., Bakken, L. R., Yavitt, J. B. & Shapleigh, J. P. Modularity
552 of nitrogen-oxide reducing soil bacteria: Linking phenotype to genotype. *Environ.*
553 *Microbiol.* **19**, 2507–2519 (2017).
- 554 20. Pihlatie, M., Syväsalo, E., Simojoki, A., Esala, M. & Regina, K. Contribution of
555 nitrification and denitrification to N₂O production in peat, clay and loamy sand soils
556 under different soil moisture conditions. *Nutr. Cycl. Agroecosystems* **70**, 135–141
557 (2004).
- 558 21. Palmer, K. & Horn, M. A. Actinobacterial nitrate reducers and Proteobacterial
559 denitrifiers are abundant in N₂O-metabolizing peat. *Appl. Environ. Microbiol.* **78**,
560 5584–5596 (2012).
- 561 22. Sanford, R. A. *et al.* Unexpected nondenitrifier nitrous oxide reductase gene diversity
562 and abundance in soils. *Proc. Natl. Acad. Sci. USA* **109**, 19709–19714 (2012).
- 563 23. Jones, C. M. *et al.* Recently identified microbial guild mediates soil N₂O sink capacity.
564 *Nat. Clim. Change* **4**, 801–805 (2014).
- 565 24. Hallin, S., Philippot, L., Löffler, F. E., Sanford, R. A. & Jones, C. M. Genomics and
566 Ecology of Novel N₂O-Reducing Microorganisms. *Trends Microbiol.* **26**, 43–55 (2018).
- 567 25. Lycus, P. *et al.* A bet-hedging strategy for denitrifying bacteria curtails their release of
568 N₂O. *Proc. Natl. Acad. Sci. USA* **115**, 11820–11825 (2018).
- 569 26. Burns, L. C., Stevens, R. J. & Laughlin, R. J. Determination of the simultaneous
570 production and consumption of soil nitrite using ¹⁵N. *Soil Biol. Biochem.* **27**, 839–844
571 (1995).
- 572 27. Burns, L. C., Stevens, R. J. & Laughlin, R. J. Production of nitrite in soil by
573 simultaneous nitrification and denitrification. *Soil Biol. Biochem.* **28**, 609–616 (1996).
- 574 28. Wullstein, L. H. & Gilmour, C. M. Non-enzymatic formation of nitrogen gas. **210**, 1150–
575 1151 (1966).
- 576 29. Liu, S., Schloter, M., Hu, R., Vereecken, H. & Brüggemann, N. Hydroxylamine
577 contributes more to abiotic N₂O production in soils than nitrite. *Front. Environ. Sci.* **7**, 1–
578 10 (2019).
- 579 30. Thorn, K. A. & Mikita, M. A. Nitrite fixation by humic substances nitrogen-15 nuclear
580 magnetic resonance evidence for potential intermediates in chemodenitrification. *Soil*
581 *Sci. Soc. Am. J.* **64**, 568–582 (2000).
- 582 31. Thorn, K. A., Younger, S. J. & Cox, L. G. Order of Functionality Loss during
583 Photodegradation of Aquatic Humic Substances. *J. Environ. Qual.* **39**, 1416–1428
584 (2010).
- 585 32. Klüpfel, L., Piepenbrock, A., Kappler, A. & Sander, M. Humic substances as fully
586 regenerable electron acceptors in recurrently anoxic environments. *Nat. Geosci.* **7**, 195–
587 200 (2014).
- 588 33. Lovley, D. R. & Blunt-Harris, E. L. Role of humic-bound iron as an electron transfer
589 agent in dissimilatory Fe(III) reduction. *Appl. Environ. Microbiol.* **65**, 4252–4254
590 (1999).
- 591 34. Kappler, A., Benz, M., Schink, B. & Brune, A. Electron shuttling via humic acids in
592 microbial iron(III) reduction in a freshwater sediment. *FEMS Microbiol. Ecol.* **47**, 85–92
593 (2004).
- 594 35. Van Cleemput, O., Patrick, W. H. & McIlhenny, R. C. Nitrite decomposition in flooded
595 soil under different pH and redox potential conditions. *Soil Sci. Soc. Am. J.* **40**, 55–60
596 (1976).
- 597 36. Van Cleemput, O. & Baert, L. Nitrite: A key compound in N loss processes under acid
598 conditions? *Plant Soil* **76**, 233–241 (1984).

- 599 37. Porter, L. K. Gaseous products produced by anaerobic reaction of sodium nitrite with
600 oxime compounds and oximes synthesized from organic matter. *Soil Sci. Soc. Am. J.* **33**,
601 696–702 (1969).
- 602 38. Liu, B., Mørkved, P. T., Frostegård, Å. & Bakken, L. R. Denitrification gene pools,
603 transcription and kinetics of NO, N₂O and N₂ production as affected by soil pH. *FEMS*
604 *Microbiol. Ecol.* **72**, 407–417 (2010).
- 605 39. Palmer, K., Biasi, C. & Horn, M. A. Contrasting denitrifier communities relate to
606 contrasting N₂O emission patterns from acidic peat soils in arctic tundra. *ISME J.* **6**,
607 1058–1077 (2012).
- 608 40. Onley, J. R., Ahsan, S., Sanford, R. A. & Löffler, F. E. Denitrification by
609 *Anaeromyxobacter dehalogenans*, a common soil bacterium lacking the nitrite reductase
610 genes *nirS* and *nirK*. *Appl. Environ. Microbiol.* **84**, 1–14 (2018).
- 611 41. Sanford, R. A., Cole, J. R. & Tiedje, J. M. Characterization and Description of
612 *Anaeromyxobacter dehalogenans* gen. nov., sp. nov., an Aryl-Halo-respiring Facultative
613 Anaerobic Myxobacterium. *Appl. Environ. Microbiol.* **68**, 893–900 (2002).
- 614 42. Mohr, K. I., Zindler, T., Wink, J., Wilharm, E. & Stadler, M. Myxobacteria in high moor
615 and fen: An astonishing diversity in a neglected extreme habitat. *MicrobiologyOpen* **6**,
616 e00464 (2017).
- 617 43. Hori, T., Müller, A., Igarashi, Y., Conrad, R. & Friedrich, M. W. Identification of iron-
618 reducing microorganisms in anoxic rice paddy soil by ¹³C-acetate probing. *ISME J.* **4**,
619 267–278 (2010).
- 620 44. Kawaichi, S. *et al.* *Ardenticatena maritima* gen. nov., sp. nov., a ferric iron- and nitrate-
621 reducing bacterium of the phylum ‘*Chloroflexi*’ isolated from an iron-rich coastal
622 hydrothermal field, and description of *Ardenticatena* classis nov. *Int. J. Sys. Evol.*
623 *Microbiol.* **63**, 2992–3002 (2013).
- 624 45. Podosokorskaya, O. A. *et al.* Characterization of *Melioribacter roseus* gen. nov., sp.
625 nov., a novel facultatively anaerobic thermophilic cellulolytic bacterium from the class
626 *Ignavibacteria*, and a proposal of a novel bacterial phylum *Ignavibacteriae*. *Environ.*
627 *Microbiol.* **15**, 1759–1771 (2013).
- 628 46. Maher, B. A. & Taylor, R. M. Formation of ultrafine-grained magnetite in soils. *Nature*
629 **336**, 368–370 (1988).
- 630 47. Sanchez, P. A. *Properties and management of soils in the tropics*. (Wiley, 1976).
- 631 48. White, A. F. *et al.* Chemical weathering in a tropical watershed, Luquillo Mountains,
632 Puerto Rico: I. Long-term versus short-term weathering fluxes. *Geochim. Cosmochim.*
633 *Acta* **62**, 209–226 (1998).
- 634 49. Hall, S. J., Liptzin, D., Buss, H. L., DeAngelis, K. & Silver, W. L. Drivers and patterns
635 of iron redox cycling from surface to bedrock in a deep tropical forest soil: a new
636 conceptual model. *Biogeochemistry* **130**, 177–190 (2016).
- 637 50. Buchwald, C., Grabb, K., Hansel, C. M. & Wankel, S. D. Constraining the role of iron in
638 environmental nitrogen transformations: Dual stable isotope systematics of abiotic NO₂⁻
639 reduction by Fe(II) and its production of N₂O. *Geochim. Cosmochim. Acta* **186**, 1–12
640 (2016).
- 641 51. Grabb, K. C., Buchwald, C., Hansel, C. M. & Wankel, S. D. A dual nitrite isotopic
642 investigation of chemodenitrification by mineral-associated Fe(II) and its production of
643 nitrous oxide. *Geochim. Cosmochim. Acta* **196**, 388–402 (2017).
- 644 52. Drewer, J. *et al.* Linking nitrous oxide and nitric oxide fluxes to microbial communities
645 in tropical forest soils and oil palm plantations in Malaysia in laboratory incubations.
646 *Front. For. Glob. Change* **3**, 1–14 (2020).

- 647 53. Yvon-Durocher, G., Jones, J. I., Trimmer, M., Woodward, G. & Montoya, J. M.
648 Warming alters the metabolic balance of ecosystems. *Philos. Trans. R. Soc. B: Biol. Sci.*
649 (2010). doi:10.1098/rstb.2010.0038
- 650 54. Yvon-Durocher, G. *et al.* Reconciling the temperature dependence of respiration across
651 timescales and ecosystem types. *Nature* **487**, 472–476 (2012).
- 652 55. Jauhiainen, J., Keröjoki, O., Silvennoinen, H., Limin, S. & Vasander, H. Heterotrophic
653 respiration in drained tropical peat is greatly affected by temperature – a passive
654 ecosystem cooling experiment. *Environmental Research Letters* **9**, 105013 (2014).
- 655 56. Wang, S., Zhuang, Q., Lähteenoja, O., Draper, F. C. & Cadillo-Quiroz, H. Potential shift
656 from a carbon sink to a source in Amazonian peatlands under a changing climate. *Proc.*
657 *Natl. Acad. Sci. USA* **115**, 12407–12412 (2018).
- 658 57. Stumm, W. & Lee, G. F. Oxygenation of ferrous iron. *Ind. Eng. Chem.* **53**, 143–146
659 (1961).
- 660 58. Theis, T. L. & Singer, P. C. Complexation of iron(II) by organic matter and its effect on
661 iron(II) oxygenation. *Environ. Sci. Technol.* **8**, 569–573 (1974).
- 662 59. Wan, X. *et al.* Complexation and reduction of iron by phenolic substances: Implications
663 for transport of dissolved Fe from peatlands to aquatic ecosystems and global iron
664 cycling. *Chem. Geol.* **498**, 128–138 (2018).
- 665 60. Daugherty, E. E., Gilbert, B., Nico, P. S. & Borch, T. Complexation and redox buffering
666 of iron(II) by dissolved organic matter. *Environ. Sci. Technol.* **51**, 11096–11104 (2017).
- 667 61. Prananto, J. A., Minasny, B., Comeau, L.-P., Rudiyanto, R. & Grace, P. Drainage
668 increases CO₂ and N₂O emissions from tropical peat soils. *Glob. Change Biol.* **26**, 4583–
669 4600 (2020).
- 670 62. Stirling, E., Fitzpatrick, R. W. & Mosley, L. Drought effects on wet soils in inland
671 wetlands and peatlands. *Earth-Sci. Rev.* **210**, 1–15 (2020).
- 672 63. Hodgkins, S. B. *et al.* Tropical peatland carbon storage linked to global latitudinal trends
673 in peat recalcitrance. *Nat. Commun.* **9**, 1–13 (2018).
- 674 64. Arias, P. *et al.* Climate change 2021: The physical science basis. Contribution of
675 Working Group I to the sixth assessment report of the intergovernmental panel on
676 climate change. (2021).
- 677 65. Babbin, A. R., Bianchi, D., Jayakumar, A. & Ward, B. B. Rapid nitrous oxide cycling in
678 the suboxic ocean. *Science* **348**, 1127–1129 (2015).
- 679 66. Hamilton, S. K. & Ostrom, N. E. Measurement of the stable isotope ratio of dissolved N₂
680 in ¹⁵N tracer experiments. *Limnol. Oceanogr.-Meth.* **5**, 233–240 (2007).
- 681 67. Stumm, W. & Morgan, J. J. *Aquatic chemistry., 3rd edn (John Wiley & Sons: New York).*
682 (1996).
- 683 68. Homyak, P. M., Kamiyama, M., Sickman, J. O. & Schimel, J. P. Acidity and organic
684 matter promote abiotic nitric oxide production in drying soils. *Glob. Change Biol.* **23**,
685 1735–1747 (2017).
- 686 69. Henry, S., Bru, D., Stres, B., Hallet, S. & Philippot, L. Quantitative detection of the *nosZ*
687 gene, encoding nitrous oxide reductase, and comparison of the abundances of 16S rRNA,
688 *narG*, *nirK*, and *nosZ* genes in soils. *Appl. Environ. Microbiol.* (2006).
689 doi:10.1128/AEM.00231-06
- 690 70. Jones, C. M., Graf, D. R., Bru, D., Philippot, L. & Hallin, S. The unaccounted yet
691 abundant nitrous oxide-reducing microbial community: a potential nitrous oxide sink.
692 *ISME J.* **7**, 417–426 (2013).
- 693 71. Zhang, B. *et al.* A new primer set for clade I *nosZ* that recovers genes from a broader
694 range of taxa. *Biol. Fertil. Soils* **57**, 523–531 (2021).

- 695 72. Herbold, C. W. *et al.* A flexible and economical barcoding approach for highly
696 multiplexed amplicon sequencing of diverse target genes. *Front. Microbiol.* **6**, 8966
697 (2015).
- 698 73. Edgar, R. C. Search and clustering orders of magnitude faster than BLAST.
699 *Bioinformatics* **26**, 2460–2461 (2010).
- 700 74. Edgar, R. C. UNOISE2: Improved error-correction for Illumina 16S and ITS amplicon
701 sequencing. *bioRxiv* 081257 (2016). doi:10.1101/081257
- 702 75. Wang, Q. *et al.* Ecological patterns of *nifH* genes in four terrestrial climatic zones
703 explored with targeted metagenomics using Framebot, a new informatics tool. *mBio* **4**,
704 e00592–13 (2013).
- 705 76. Buchfink, B., Xie, C. & Huson, D. H. Fast and sensitive protein alignment using
706 DIAMOND. *Nat. Methods* **12**, 59–60 (2015).
- 707 77. Fish, J. A. *et al.* FunGene: the functional gene pipeline and repository. *Front. Microbiol.*
708 **4**, 1–14 (2013).
- 709 78. Huson, D. H. *et al.* MEGAN Community Edition - Interactive exploration and analysis
710 of large-scale microbiome sequencing data. *PLoS Comput. Biol.* **12**, e1004957 (2016).
- 711 79. Huson, D. H. *et al.* MEGAN-LR: New algorithms allow accurate binning and easy
712 interactive exploration of metagenomic long reads and contigs. *Biol. Direct* **13**, 1–17
713 (2018).
- 714 80. Ondov, B. D., Bergman, N. H. & Phillippy, A. M. Interactive metagenomic visualization
715 in a Web browser. *BMC Bioinform.* **12**, 1–10 (2011).
- 716 81. Kumar, S., Stecher, G., Li, M., Knyaz, C. & Tamura, K. MEGA X: Molecular
717 evolutionary genetics analysis across computing platforms. *Mol. Biol. Evol.* **35**, 1547–
718 1549 (2018).
- 719

720 **Data availability**

721 All data to evaluate the conclusions of the study are present in the paper and the Supplementary
722 Information.

723

724 **Acknowledgments**

725 We acknowledge Dr. Rodil Tello Espinoza, Dr. Tedi Pacheco Gomez, David Reyna, Brian
726 Crnobrna, Dr. Outi Lahteenoja, Kelsen Arbaiza, Antenor Hurtado Carmona, Paulo Fonteboa,
727 Ronaldo Cesar Chaves, Juan Rodrigo Trucios, Cely Mariela Cadillo-Quiroz, the UFSJ Graduate
728 Program in Geography (PPGEOG) and Office for International Affairs (ASSIN/UFSJ) for
729 assistance and help during stages of field work. We also thank Wolfgang Nitschke (CNRS/BIP)
730 for discussions and Mohamed Abdalla for his work supporting this effort at the USAID-GDR
731 program at ASU.

732 This study was primarily funded by an NSF-DEB award (#1355066) and a SOLS -KED ASU
733 award (ECR A548 HC) to H.C-Q, a Global Development Research Scholarship to S.B. and
734 H.C-Q in partnership with the USAID-Global Development Lab and Peruvian and Brazilian
735 USAID missions. S.B. also received support by the Lewis & Clark Fund for Exploration and
736 Field Research in Astrobiology provided by the American Philosophical Society (APS). N.E.O.
737 was funded in part by the DOE Great Lakes Bioenergy Research Center (DOE BER Office of
738 Science DE-SC0018409).

739

740 **Author contributions**

741 S.B., N.E.O., and H.C.-Q. designed the study. S.B. conducted the field work with essential
742 contributions from A.G.P-C, G.P.P., J.D.U.-M., L.P.R., J.M.F.M., I.G.B., and B.G.. S.B.,
743 M.F.O., A.F.S., and M.C. R. performed laboratory experiments and molecular analyses. S.J.H.
744 supported the NO analysis. K.E.H. conducted soil gamma sterilization. C.R.P. supported qPCR
745 analysis. H.G. analyzed isotopic abundances of gas samples. S.B., I.G.B., B.G., N.E.O., and
746 H.C.-Q. performed the data analysis. S.B. and H.C.-Q. wrote the manuscript, and all co-authors
747 contributed to the final version of the paper.

748

749 **Competing interests**

750 The authors have no competing interests to declare.